International Journal of GEOMATE, June., 2021, Vol.20, Issue 82, pp.140-145
ISSN: 2186-2982 (P), 2186-2990 (O), Japan, DOI: https://doi.org/10.21660/2021.82.j2017
Geotechnique, Construction Materials and Environment

SEISMIC DEFORMATION BEHAVIOUR OF SEGMENTAL GEOGRID REINFORCED SOIL WALL

*Albano Ajuda[1] and Jiro Kuwano[2]

Saitama University, Japan [1,2]

*Corresponding Author, Received: 20 Oct. 2020, Revised: 25 Feb. 2021, Accepted: 10 Mar. 2021

ABSTRACT: This paper presents results from a series of 1g shaking table tests on seismic deformation behaviour of segmental geogrid reinforced soil walls using multiple reinforcement stiffness along the wall. The reinforcement stiffness arrangement along the wall height was uniform, alternating and grouped schemes. During the experimental program, digital image analysis technique was employed to capture the failure mechanism and distribution of shear strains in the backfill. It was found that the facing wall deformation strongly depends on the reinforcement stiffness arrangement. The deformation of the models consisted of overturning, sliding, and bulging. By constructing walls with alternating reinforcement stiffness, similar deformation behaviour compared to uniform reinforcement stiffness was observed. However, placing weak reinforcement stiffness either in the upper half or lower half of the wall height, large deformation occurred in these locations, and bulging deformation was observed. The shear strains were also dependent on the reinforcement arrangement prior to critical acceleration. The highest values of shear strains were observed in walls constructed in a grouped arrangement.

Keywords: Earthquake, Shaking table, Deformations, Shear Strains, Geogrids

1. INTRODUCTION

Geosynthetics reinforced soil walls (GRS) have been used in many civil engineering projects worldwide due to improved seismic performance and cost-effective compared to conventional retaining walls such as gravity and cantilever-type. Many of the constructed GRS walls demonstrated very high seismic stability from previously recorded earthquakes. For example, Kuwano et al. [1], reported that during the Tohoku earthquake, 90% of the reinforced soil walls showed no damage despite a massive tsunami accompanied the earthquake. Investigation on the seismic performance of GRS walls has been carried out by many researchers using the shaking table [2-8]. However, most of the existing studies focus on applying a uniform reinforcement stiffness along with the GRS wall height. Matsuo et al. [8] showed that increasing the ratio of geogrid length to the wall height from 0.4 to 0.7 was the most effective method to reduce wall deformation.

Some attempts have been made to improve stability while reducing the total construction cost by combining different reinforcement materials along with the GRS wall height. Leshchinsky [9] introduced the concept of hybrid GRS walls, consisting of shorter reinforcement in between longer reinforcement. They reported that with shorter reinforcement, it is possible to reduce the longer reinforcement's connection force, increase internal stability, and reduce the down-drag effect. Jiang [10] investigate the effect of the inclusion of secondary reinforcement stiffness and length using a numerical method. It was reported that the facing displacement decreased with an increase in the secondary reinforcement length and stiffness. An increase in the reinforcement stiffness can reduce the maximum tensile stress and connection stress of the primary reinforcement.

Lelli et al. [11] showed a case study of hybrid reinforce soil wall constructed in India, Albania, and Turkey. The walls were constructed using geogrid as a primary reinforcement and steel wires as secondary reinforcement. They reported that the choice was that the walls have more permeability and are const-effective to conventional GRS walls. Watanabe et al. [7] reported that placing longer reinforcement near the top of the wall can substantially increase overturning resistance. In the current experimental program, a series of 1g shaking table test was conducted to investigate the GRS wall's failure mechanism using different reinforcement stiffness and the wall height in different arrangements. During the experimental program, the facing lateral deformation and backfill deformation were monitored using a digital image analysis technique.

2. TEST SETUP

A computer-controlled shaking table test was used to simulate seismic loading. The experimental program was conducted at Saitama University, Japan. The shaking table test was constructed on a plan dimension of 1,300 (L) by 1,000 (W) seated on

a pair of low friction bearing rails constrained to the horizontal direction equivalent to a single degree of freedom.

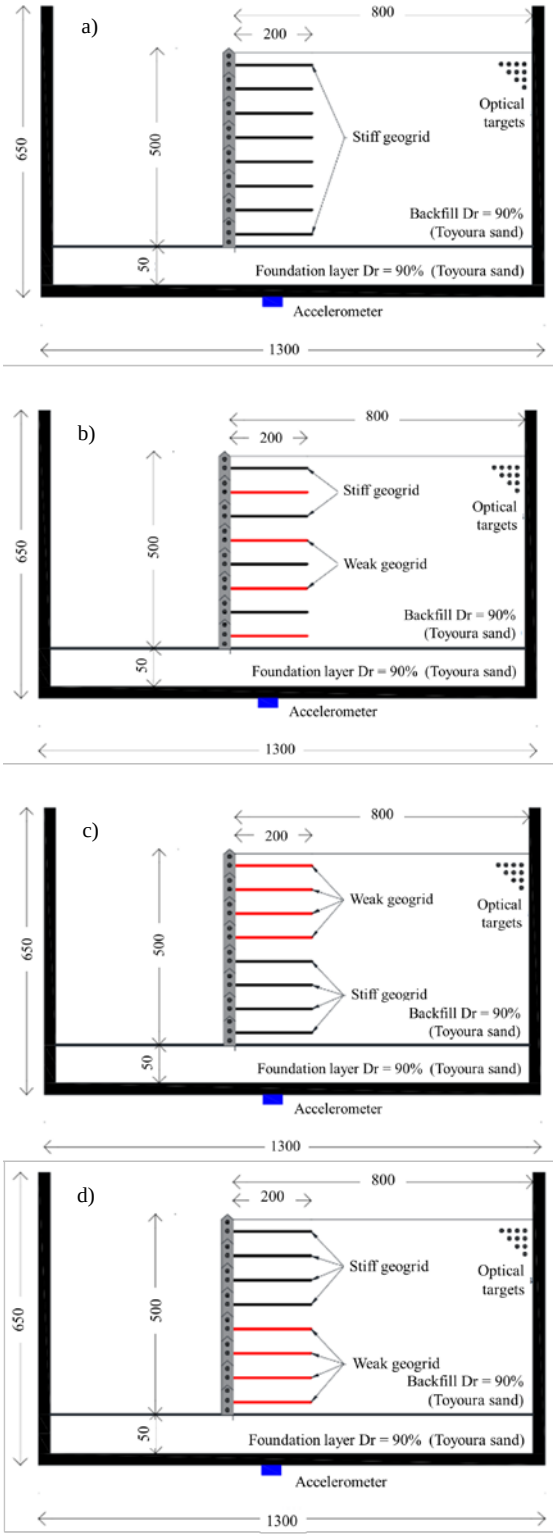

Fig. 1 Summary of testing program a) test 1, b) test 2, c) test 3 and d) test 4.

The soil was poured in a rigid steel container built with the following dimension: 1,300 mm (long), 600 mm (wide), and 650 mm (high). One side of the soil container was constructed with a transparent Plexiglas to visualize the wall and backfill deformation during model testing. The rigid box was sufficiently rigid to keep plane strain conditions in the reduced-model. The Iai [12] similitude rules for shaking table models between model and prototype was used in the present research a geometric scale of 1/10 was adopted in the present study. Fig. 1 shows the summary of tested cases.

Pre-cast concrete facing panels are commonly used in Japan. Therefore, in the present research work, the wall models were modeled as segmental walls with a total height of 500 mm, divided into a total of eight wall panels stacked on top of each other without an additional connection so they can rotate against each other as shown in Fig. 2. The wall panels were built with a lightweight acrylic material; in both sides of each wall panels, Teflon sheets with the same height as the wall panels were glued in the lateral sides of the wall panels to minimize friction between the rigid container as well to prevent any sand leakage during the model test. Soil (Toyoura sand) was used to prepare the soil foundation as well as the backfill. The sand layer was prepared by using a sand hopper and keeping a falling height of sand particles constant. The average relative density for both foundation and backfill was 90 % achieved using this method.

Two types of biaxial geogrids with 200 mm long were used for the reinforcement layers, as shown in Fig. 2. The first reinforcement type is made of a stiff polypropylene (PP) geogrid, and the second was made of a weak and flexible geogrid, which is not commercially available for reinforced soil application was used only for experimental purposes in simulating the low reinforcement stiffness. The geogrid reinforcement was clapped using bolts and nuts between two steel plates with the same length as the wall panels. This type of connection was designed to prevent the slippage of the geogrid during model testing. To obtain the displacement and shear strains, digital image analysis was employed in the shaking table tests. A series of optical targets were placed in the backfill as well in contact with the plexiglass. The displacement of the targets allowed to observe the geometry and failure mechanism of the model test. The camera was mounted in a special design frame attached to the shaking table test to vibrate at the same phase, eliminating the need for additional correction. The resulting displacement is units of pixels; therefore, calibration is required to convert into (cm). This is achieved by placing a series of permanent targets whose position is known relatively to the container.

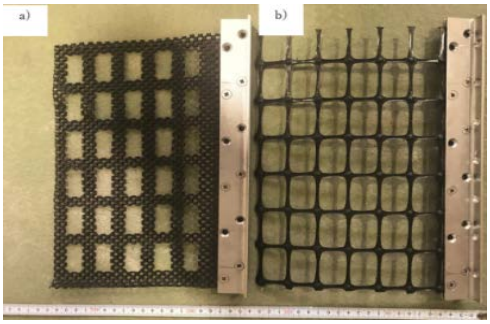

Fig. 2 Model reinforcement a) weak and b) stiff geogrids.

In this experimental program, a sinusoidal wave was applied to each test case with a predominant 5 Hz frequency, as illustrated in Fig. 3. The seismic motion was applied incrementally from 1 m/s^2 with a steady increment of acceleration amplitude of 1 m/s^2 until the models fully collapsed or measurement was impossible, each shaking stage was held for 10 seconds corresponding to 50 cycles each stage. This simple waveform was chosen to generate large facing and backfill lateral deformation

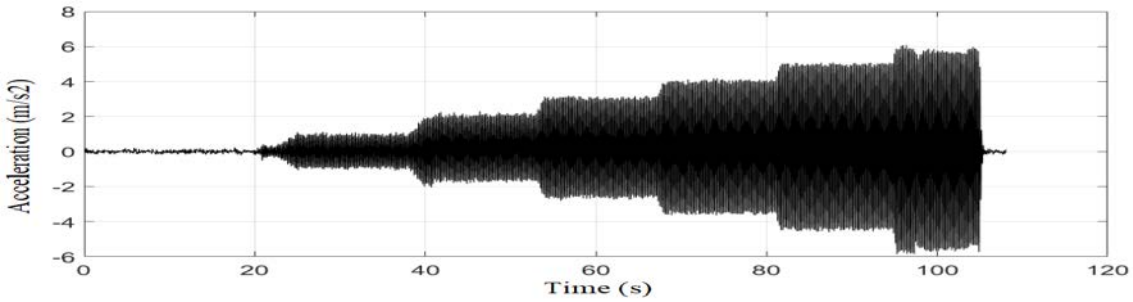

Fig. 3 Input seismic motion

3. RESULTS AND DISCUSSION

3.1. Seismic Facing Displacement

Fig. 4 shows the relationship between the top facing lateral displacement with base input acceleration. It can be seen that the top displacement increases steadily until some critical acceleration; at this point, the active wedge of failure was formed in the backfill, which then generates a sharp increase in the top lateral displacement towards the catastrophic collapse. The critical acceleration and development of the active wedge of failure were observed when the top displacement reached a value of 3% of the total wall height. A similar observation is reported by Izawa and Kuwano [4]. Moreover, it should be noted that in test 3 and test 4, before the critical acceleration, it was observed intense bulging deformation of the facing wall, as discussed in the following section.

Fig. 5 shows the relationship between the facing elevation and lateral deformation. In can be observed that in test 1 the deformation is linear, extending from the toe of the GRS wall towards the top. It is also possible to observed sliding and overturning components about 0.04 cm and 0.07 cm, respectively. In test 2, the deformation pattern and the amount of lateral deformation were the same as in test 1.

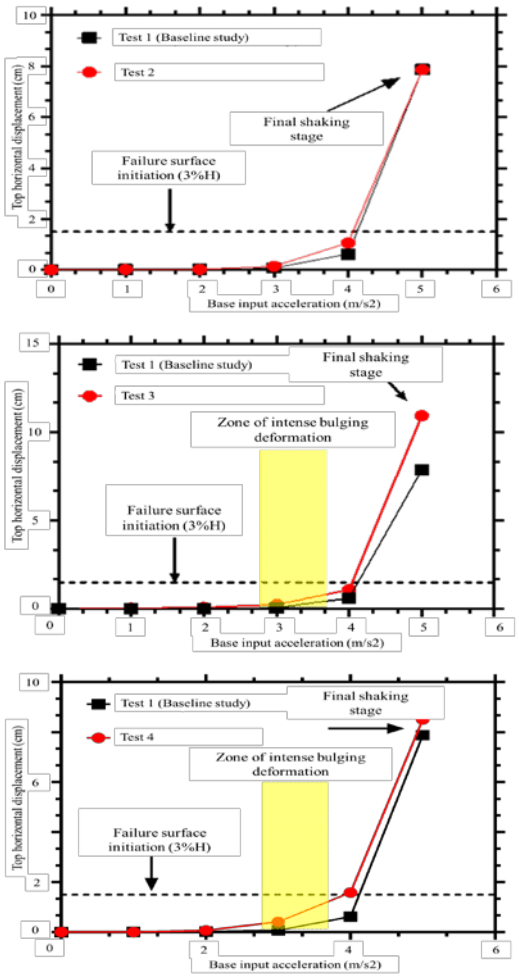

Fig. 4 Relationship between top displacement and base acceleration.

However, in test 3 and test 4, the difference is noticeable. The first portion of the wall constructed with only stiff geogrid sliding can be observed, and then at mid-height, where the reinforcement is changed to weak geogrid, there is an increase in facing lateral deformation leading to a concave type deformation. In test 4, the wall deforms with convex shape deformation; the maximum lateral deformation is also recorded at mid-height. It can be concluded that constructing the GRS wall with multiple stiffnesses in an alternating arrangement can be a practical cost reduction approach. Moreover, it can be observed that the maximum displacement is recorded in locations where the weak geogrid is placed.

3.2. Seismic Failure Mechanism

Fig. 6 shows the failure mechanism in all tests. In general, it was found that irrespective of the reinforcement stiffness arrangement, the failure process was the same. Prior to any shaking, the models were stable, and no evidence of lateral deformation is recorded. After applying seismic waves, failure surfaces appeared from the top of the backfill in the interface between reinforced and unreinforced zone. As the wall continued t rotate to the outward direction, an inclined failure surface appeared from the backfill surface in the unreinforced zone and moved downwards towards the end of the last geogrid layer (counting from the top), and after the GRS wall reached the failure stage, a new inclined failure surface appeared in the reinforced zone intersecting the toe of the wall. Despite multiple reinforcement stiffness and the GRS wall height, the failure surfaces observed in the present models during the shaking table test remained the same at the failure. For instance, Izawa and Kuwano [4], investigated the behavior of geogrid reinforced soil walls subjected to pseudo-static loading using a centrifuge tilting table test together with a two-wedge analysis. It was reported that failure surfaces have different geometries under different geogrid tensile strength. To conclude, the failure surface behavior observed in the present study suggests that despite multiple reinforcement stiffness along with the reinforced soil wall system, the failure surface angle will be governed by its reinforcement length and the highest reinforcement stiffness.

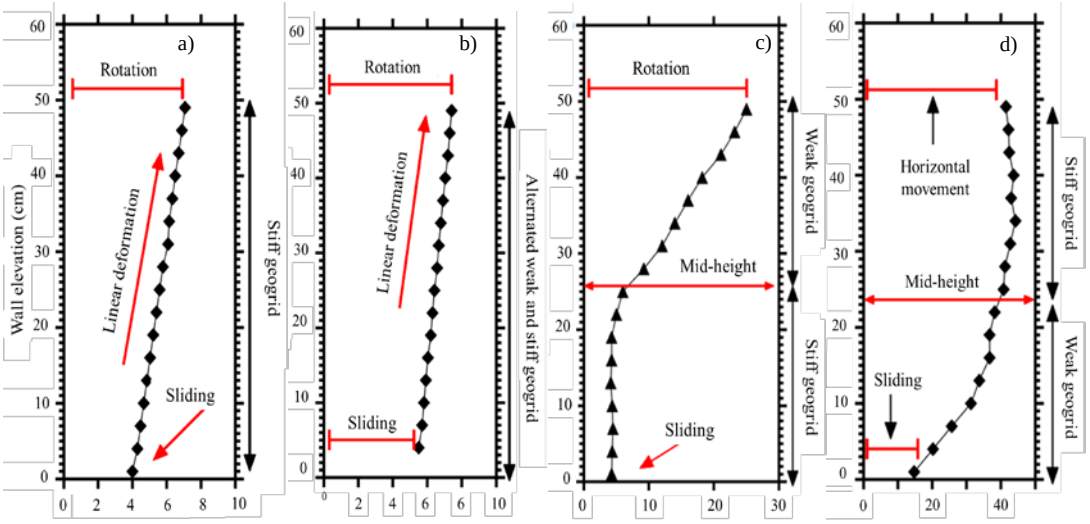

Fig. 5 Relationship between wall elevation and lateral deformation a) test 1, b) test 2, c) test 3 and d) test 4.

3.3. Distribution of Shear Strains

The shear strain contour was obtained at the corresponding critical acceleration of 3% of the wall height as shown in Fig 6. It is possible to notice that maximum shear strain depends on the reinforcement stiffness arrangement during critical acceleration. The magnitude of the maximum shear strain of Test 1 was much less than the rest of the tested cases, as it is more able to prevent the shear deformation owing to the stiff reinforcement layers, followed by Test 2. However, grouped reinforcement stiffness walls, Test 3 and Test 4 showed a large backfill movement, consequently, increased magnitude of shear strain along the failure surfaces attributed to bulging deformation observed before the critical acceleration as shown in Fig. 4. For Test 1, Test 2, and Test 3, the formation of the active failure wedge was induced mainly by the large rotation of the wall top and sliding of the base, while in Test 3 and Test 4 the activation of the active failure surface is attributed to the sliding and bulging mechanism which was more predominant.

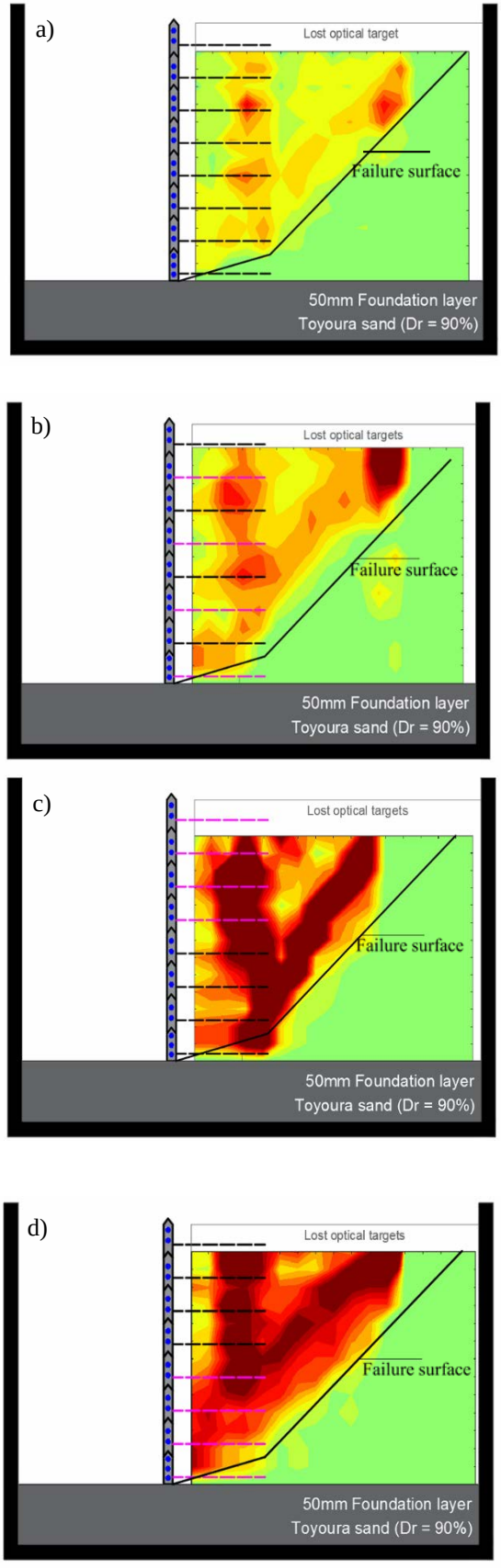

Fig 6. Distribution of maximum shear strains a) Test 1, b) Test 2, and c) Test 3 d) Test 4.

4. CONCLUSIONS

The present paper presents results from a series of 1g shaking table tests to investigate the failure mechanism of segmental geosynthetic reinforced soil wall constructed with two types of geogrids in different arrangements and wall height. The following is a summary of the test results: Irrespective of the reinforcement stiffness arrangement along with the wall height, the failure mechanism and failure surface angles remained the same, with a two-wedge geometry; The critical acceleration and development of the active wedge of failure was found at 3% of the wall height for all cases. Moreover, by alternating the reinforcement stiffness along with the wall height, the facing and backfill deformation was similar. By grouping the weak reinforcement, either in the upper or lower part of the facing wall, bulging deformation was observed, and the maximum deformation occurred in the location where the weak reinforcement is placed.

5. ACKNOWLEDGMENTS

This research was support by KAKENHI GRANT number 16H04406.

6. REFERENCES

[1] Kuwano J., Miyata Y. and Koseki J., "Performance of reinforced soil walls during the 2011 Tohoku earthquake," Geosynthetics International, 2014, pp. 389-402.

[2] Anastasopoulos I., Georgarakos T., Georgiannou V., Drosos V. and Kourkoulis R., "Seismic performance of bar-mat reinforced-soil retaining wall: Shaking table testing versus numerical analysis with modified kinematic hardening constitutive model," 2010, Vol. 30, No. 10, pp. 1089-1105.

[3] El-Emam M. M. and Bathrust R. J., "Experimental Design, instrumentation and Interpretation of Reinforced Soil Wall Response Using a Shaking Table Test," International Journal of Physical Modelling in Geotechnics , Vol. 4, No. 4, 2004, pp. 13-32,.

[4] Izawa J. and Kuwano, J., "Evaluation of extent of damage to geogrid reinforced soil walls subjected to earthquakes," Soils nad Foundations, Vol. 51, No. 5, 2011, pp. 945-958.

[5] Xu P., Hatami K. and Jiang G. " Study on seismic stability and performance of reinforced soil walls using shaking table tests," Geotextiles and Geomembranes, Vol. 48, No. 1, 2020, pp. 82-97.

[6] Ling H. I., Mohri Y. and Burke C., "Large-scale shaking table test on modular block

reinforced soil retaining walls," Journal of geotechnical and geoenviromental engineering, Vol. 131, No. 4, 2005.

[7] Watanabe K., Munaf Y., Koseki J., Tateyama M. and Kojima K., "Behaviour of Several Types of Model Retaining Walls Subjected to Irregular Excitation," Soils and Foundations, Vol. 43, No. 5, 2003.

[8] Matsuo O., Yokoyama K. and Saito Y., "Shaking table tests and analysis of geosynthetic-reinforced soil retaining walls," Geosynthetics International, Vol.5, No. 1-2, 1998, pp. 97-126.

[9] Leshchinsky D., "Alleviating connection load," Geotechnical Fabrics Report, 2000.

[10] Jiang Y., Evaluating Performance of Hybrid Geosynthetic-Reinforced Retaining Walls, PhD Thesis, Univerisity of Kansas, 2016.

[11] Lelli M., Laneri R. and Rimoldi P., "Innovative reinforced soil structure for high walls and slopes combining polymeric and metallic reinforcements," in The 5th International conference of Euro Asia Civil Engineering Forum (EACEF-5), 2015.

[12] Iai S. "Similitude for shaking table tests on soil-structure-fluid model in 1g gravitational field," Soils and Foundations, Vol. 29, No. 1, 1989, pp. 105-118.

[13] Izawa J. and Kuwano J., "Centrifuge modelling of geogrid reinforced soil walls subjected to pseudo-static loading," International Journal of Physical Modelling in Geotechnics, Vol. 10, No. 1, 2010, pp. 1-18.